Columnar Mesophases from Nondiscoid Metallomesogens: Rhodium and Iridium Dicarbonyl Diketonates

Scott T. Trzaska[†,‡] and Timothy M. Swager*[,†]

Department of Chemistry, Massachusetts Institute of Technology, Cambridge, Massachusetts 02139-4307, and Department of Chemistry, University of Pennsylvania, Philadelphia, Pennsylvania 19104-6323

Received September 8, 1997. Revised Manuscript Received October 30, 1997[⊗]

A series of nondiscoid rhodium and iridium dicarbonyl β-diketonate complexes have been shown to organize in columnar liquid crystal phases with hexagonal disordered structures (Col_{hd}). The shape and dipolar attributes of these materials produce highly correlated antiparallel pairwise arrangements. This organization was investigated by X-ray diffraction and miscibility studies. The liquid crystallinity was found to be stabilized by decreasing the number of carbon atoms in the side chains, and single component room-temperature liquid crystals were developed. The nature of the metal is also important, and iridium mesogens exhibited higher clearing points than the analogous rhodium materials.

Introduction

One-dimensional stacking of metal centers has led to materials with interesting properties in the crystal phase such as magnetism and one-dimensional conductivity.[1] The ability to produce these bulk properties in metallomesogens would offer important routes to anisotropic materials that can be readily aligned in devices. An additional feature of designing liquid crystalline materials containing transition metals is that they produce molecular shapes and intermolecular interactions that are uncommon to pure organic molecules. Compounds with novel shapes can produce liquid crystalline systems with unusual and highly ordered bulk alignments as well as specific intermolecular interactions.[2]

Several nondiscoid-shaped metallomesogens have been shown to organize in columnar phases commonly observed in planar disc-shaped molecules.[3] One approach to these systems is to use molecules with shapes designed to complement each other. Of particular interest here are half-disc compounds that align as shown in Figure 1 in a highly ordered antiparallel fashion with each molecule rotated 180° with respect to its nearest neighbor. We refer to systems which align in this antiparallel correlated columnar arrangement as columnar antiphases in analogy to the well-known smectic antiphases.[4] There are other examples of metallomesogens that align in columnar antiphases reported in the literature.[3c] Herein we report rhodium and iridium dicarbonyl β-diketonates (**1** and **2**) that assemble into columnar antiphases.

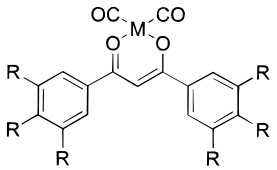

R = O $(CH_2)_n$H
1 M = Rh
2 M = Ir

Compounds **1** and **2** were of interest due to the properties associated with the analogous crystalline acetylacetonate systems. Both the rhodium and iridium dicarbonyl acetylacetonates have been reported to crystallize in a strict antiparallel arrangement that positions the metal centers on top of each other to produce a one-dimensional chain structure as shown in Figure 2.[5] This arrangement is similar to the columnar antiphase configuration observed previously for nondiscoid-shaped liquid crystals.[3c] In the rhodium and iridium acetylacetonate systems, the extended interactions are the result of metal−metal σ bonding between the square planar d^8 transitional metal complexes. The weak σ bonding interactions are formed between occupied dz^2 and unoccupied pz orbitals and result in anisotropic semiconductive and piezoresistive properties.[1,6] It was

[†] Massachusetts Institute of Technology.
[‡] University of Pennsylvania.
[⊗] Abstract published in *Advance ACS Abstracts,* December 15, 1997.

(1) Miller, J. S.; Epstein, A. J. In *Progress in Inorganic Chemistry*; Lippard, S. J., Ed.; John Wiley and Sons: New York, 1976; Vol. 20.
(2) (a) Serrette, A.; Carroll, P. J.; Swager, T. M. *J. Am. Chem. Soc.* **1992**, *114*, 1887. (b) Xu, B.; Swager, T. M. *J. Am. Chem. Soc.* **1993**, *115*, 1659. (c) Zheng, H.; Swager, T. M. *J. Am. Chem. Soc.* **1994**, *116*, 761.
(3) (a) Lai, C. K.; Serrette, A.; Swager, T. M. *J. Am. Chem. Soc.* **1992**, *114*, 7948. (b) Serrette, A.; Swager, T. M. *J. Am. Chem. Soc.* **1993**, *115*, 8879. (c) Zheng, H.; Lai, C. K.; Swager, T. M. *Chem. Mater.* **1994**, *6*, 101. (d) Atencio, R.; Barberá, J.; Cativiela, C.; Lahoz, F. J.; Serrano, J. L.; Zurbano, M. M. *J. Am. Chem. Soc.* **1994**, *116*, 11558. (e) Ohta, K.; Morizumi, Y.; Akimoto, H.; Takenaka, O.; Fujimoto, T.; Yamamoto, I. *Mol. Cryst. Liq. Cryst.* **1992**, *214*, 143.
(4) Gray, G. W.; Goodby, J. W. G. *Smectic Liquid Crystals: Textures and Structures*; Leonard Hill Publishers: Glasgow, 1984; pp 143−149.
(5) (a) Ballard, L. F.; Wortman, J. J. *J. Appl. Phys.* **1970**, *41*(10), 4232. (b) Bailey, N. A.; Coates, E.; Robertson, G. B.; Bonati, F.; Ugo, R. *J. Chem. Soc. Chem. Commun.* **1967**, *20*, 1041.

S0897-4756(97)00609-1 CCC: $15.00
Published on Web 01/19/1998

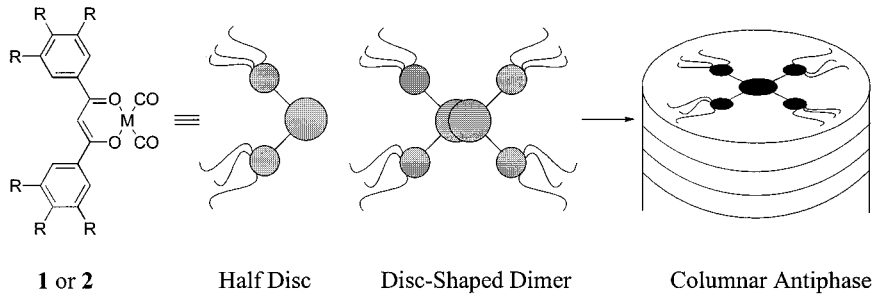

Figure 1. Illustration depicting how a columnar mesophase can be formed by a nondiscoid-shaped molecule.

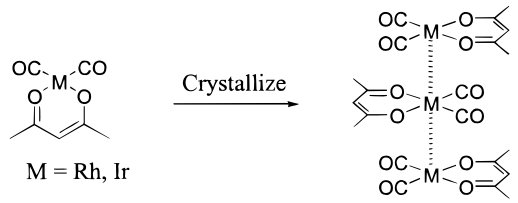

Figure 2. Depiction illustrating the alignment of rhodium and iridium dicarbonyl acetylacetonate in the crystal phase.

hoped that the liquid crystal phases of **1** and **2** could support similar interactions to produce novel extended one-dimensional electronic structures. The design of a liquid crystalline half-disc compound would be advantageous for increasing the degree of metal−metal interactions in such a system with a decreased steric environment around the metal center compared to a disc-shaped compound.

Results and Discussion

The β-diketonate ligands were synthesized by condensation reactions between alkoxy acetophenones with the appropriate esters as previously reported.[7] The rhodium and iridium dicabonyl β-diketonate compounds were prepared using modifications of procedures previously reported in the literature.[8,9] Tetracarbonyldi-μ-chlorodirhodium (I) was reacted with β-diketonate ligands in the presence of excess potassium carbonate to give rhodium dicarbonyl β-diketonates. The iridium dicarbonyl β-diketonate compounds required an indirect synthesis by first making the analogous cyclooctadiene compound by reacting chloro-1,5-cyclooctadieneiridium-(I) dimer with β-diketonate ligands in the presence of excess potassium carbonate or potassium hydroxide. The resulting iridium 1,5-cyclooctadiene β-diketonates were transformed to the respective dicarbonyl compounds by bubbling carbon monoxide through tetrahydrofuran solutions, which displaced the cyclooctadiene from the iridium center.

The metal dicarbonyl β-diketonates were moderately air sensitive. They could be handled for brief periods of time at room temperature in the atmosphere. However, the compounds decomposed in solution or at elevated temperatures when exposed to the atmosphere.

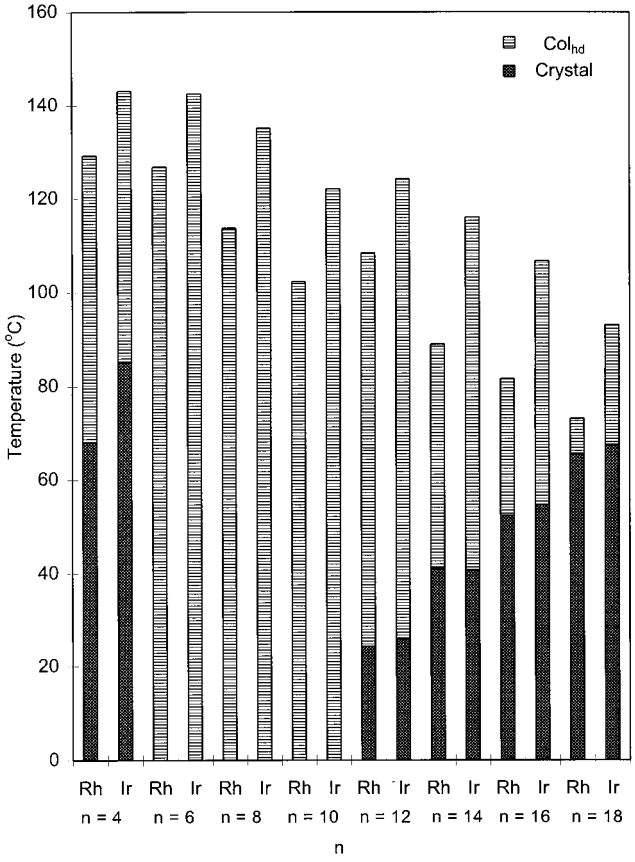

Figure 3. Bar graph showing the phase behavior of the rhodium complexes (**1**) and the iridium complexes (**2**). Note the consistently higher clearing temperatures for the iridium complexes.

In an attempt to decrease the steric environment around the metal core, rhodium and iridium dicarbonyl β-diketonates with one, three, and four alkoxy side chains (**3**−**8**) were synthesized. However, these compounds were not liquid crystalline. Enantiotropic liquid crystal phases were observed over a wide temperature range as shown in Figure 3 when the number of alkoxy side chains was increased to six (**1** and **2**). This class of compounds was found to display mesomorphism with side chain lengths of 4, 6, 8, 10, 12, 14, 16, and 18 carbon atoms. Compounds with an odd number of carbon atoms in the side chains were not investigated.

The range of stability displayed by the mesophase was found to be dependent on the number of carbon atoms in the side chains of **1** and **2**. The observed decrease in the clearing point accompanying an increase in side

(6) (a) Pitt, C. G.; Monteith, L. K.; Ballard, L. F.; Collman, J. P.; Morrow, J. C.; Roper, W. R.; Ulkü, D. *J. Am. Chem. Soc.* **1966**, *88*, 4286. (b) Interrante, L. V.; Bundy, F. P. *Inorg. Chem.* **1971**, *10*, 1169. (c) Mann, K. R.; Gordon, J. G., II; Gray, H. B. *J. Am. Chem. Soc.* **1975**, *97*, 3553. (d) Novoa, J. J.; Aullón, G.; Alemany, P.; Alvarez, S. *J. Am. Chem. Soc.* **1995**, *117*, 7169. (e) Connick, W. B.; Marsh, R. E.; Schaefer, W. P.; Gray, H. B. *Inorg. Chem.* **1997**, *36*, 913.

(7) (a) Serrette, A. G.; Lai, C. K.; Swager, T. M. *Chem. Mater.* **1994**, *6*, 2252. (b) Zheng, H.; Lai, C. K.; Swager, T. M. *Chem. Mater.* **1995**, *7*, 2067.

(8) Bonati, F.; Wilkinson, G. *J. Chem. Soc.* **1964**, 3150.

(9) Whitmore, B. C.; Eisenberg, R. *Inorg. Chem.* **1984**, *23*, 1697.

Table 1. Phase Behavior of 1[a]

compd	*n*	phase behavior
1	4	K $\underset{35.8\ (-2.46)}{\overset{68.1\ (6.47)}{\rightleftharpoons}}$ Col_{hd} $\underset{124.0\ (-0.35)}{\overset{129.3\ (0.88)}{\rightleftharpoons}}$ I
	6	Col_{hd} $\underset{101.9\ (-0.33)}{\overset{126.8\ (0.47)}{\rightleftharpoons}}$ I
	8	Col_{hd} $\underset{108.7\ (-0.80)}{\overset{113.7\ (0.79)}{\rightleftharpoons}}$ I
	10	Col_{hd} $\underset{98.1\ (-0.59)}{\overset{102.2\ (0.76)}{\rightleftharpoons}}$ I
	12	K $\xrightarrow{24.27\ (6.89)}$ Col_{hd} $\underset{98.0\ (-0.72)}{\overset{103.1\ (0.89)}{\rightleftharpoons}}$ I
	14	K $\underset{36.5\ (-11.34)}{\overset{41.0\ (11.00)}{\rightleftharpoons}}$ Col_{hd} $\underset{82.9\ (-0.67)}{\overset{89.0\ (0.54)}{\rightleftharpoons}}$ I
	16	K $\underset{45.7\ (-15.1)}{\overset{52.3\ (16.38)}{\rightleftharpoons}}$ Col_{hd} $\underset{74.4\ (-0.60)}{\overset{81.6\ (0.73)}{\rightleftharpoons}}$ I
	18	K $\underset{59.4\ (-16.54)}{\overset{65.5\ (20.12)}{\rightleftharpoons}}$ Col_{hd} $\underset{63.2\ (-0.38)}{\overset{73.1\ (0.26)}{\rightleftharpoons}}$ I

[a] The transition temperatures (°C) and enthalpies, in parentheses (kcal/mol), were determined by DSC (scan rate 10 °C/min) and are given above and below the arrows. The number of carbon atoms in the alkyl chain is represented by *n*. The designation I, Col_{hd}, and K represent isotropic, columnar hexagonal disordered, and crystal phases, respectively.

Table 2. Phase Behavior of 2[a]

compd	*n*	phase behavior
2	4	K $\underset{31.1\ (-4.81)}{\overset{85.1\ (3.96)}{\rightleftharpoons}}$ Col_{hd} $\underset{136.1\ (-0.36)}{\overset{143.1\ (0.74)}{\rightleftharpoons}}$ I
	6	Col_{hd} $\underset{77.2\ (-0.316)}{\overset{142.5\ (0.45)}{\rightleftharpoons}}$ I
	8	Col_{hd} $\underset{127.9\ (-0.78)}{\overset{135.1\ (1.52)}{\rightleftharpoons}}$ I
	10	Col_{hd} $\underset{110.2\ (-0.26)}{\overset{122.1\ (0.35)}{\rightleftharpoons}}$ I
	12	K $\xrightarrow{25.8\ (6.94)}$ Col_{hd} $\underset{119.0\ (-1.43)}{\overset{124.1\ (1.39)}{\rightleftharpoons}}$ I
	14	K $\underset{30.8\ (-9.42)}{\overset{40.7\ (12.15)}{\rightleftharpoons}}$ Col_{hd} $\underset{111.9\ (-1.58)}{\overset{116.0\ (1.50)}{\rightleftharpoons}}$ I
	16	K $\underset{46.9\ (-15.6)}{\overset{54.6\ (22.4)}{\rightleftharpoons}}$ Col_{hd} $\underset{101.6\ (-1.28)}{\overset{106.7\ (1.13)}{\rightleftharpoons}}$ I
	18	K $\underset{57.9\ (-18.5)}{\overset{65.3\ (33.6)}{\rightleftharpoons}}$ Col_{hd} $\underset{87.0\ (-0.69)}{\overset{93.2\ (0.66)}{\rightleftharpoons}}$ I

[a] All labels and details are as described for Table 1.

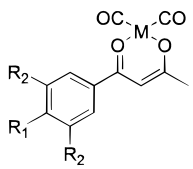

R_1 = O $(CH_2)_nH$
R_2 = H
3 M = Rh
4 M = Ir

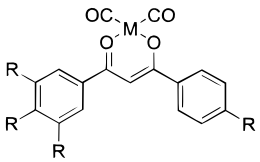

R_1 = R_2 = O $(CH_2)_nH$
5 M = Rh
6 M = Ir

R = O $(CH_2)_nH$
7 M = Rh
8 M = Ir

chain length can be attributed to the greater dispersive forces present with longer side chains. The higher clearing point observed when M = iridium (see Tables 1 and 2) is likely due to the greater radial extension of the $5dz^2$ orbital in iridium over the $4dz^2$ orbital in rhodium and/or greater dipolar interactions between the iridium complexes.

Table 3. Variable-Temperature XRD for 1

n	mesophase	lattice constant (Å)	spacing obsd	Miller indices	Å (calcd)	halos obsd
4	Col_{hd} at 90 °C	19.31	16.72	100		7.24
						3.67
6	Col_{hd} at 23 °C	22.38	19.38	100		7.25
						4.53
						3.65
8	Col_{hd} at 23 °C	23.96	20.75	100		7.07
						4.61
						3.58
10	Col_{hd} at 23 °C	25.99	22.51	100		7.17
			13.18	110	(13.00)	4.63
			11.22	200	(11.26)	3.61
12	Col_{hd} at 60 °C	28.22	24.44	100		7.29
			14.14	110	(14.11)	4.63
			12.35	200	(12.22)	3.69
14	Col_{hd} at 60 °C	29.65	25.68	100		7.08
			14.93	110	(14.83)	4.57
			12.95	200	(12.84)	3.71
16	Col_{hd} at 60 °C	30.81	26.68	100		7.24
			15.57	110	(15.40)	4.58
			13.55	200	(13.34)	3.70
18	Col_{hd} at 68 °C	33.91	29.37	100		4.52
			17.03	110	(16.96)	3.64
			14.79	200	(14.69)	

Table 4. Variable-Temperature XRD for 2

n	mesophase	lattice constant (Å)	spacing obsd	Miller indices	Å (calcd)	halos obsd
4	Col_{hd} at 120 °C	19.53	16.91	100		7.12
						3.78
6	Col_{hd} at 23 °C	21.51	18.63	100		7.08
						3.85
8	Col_{hd} at 23 °C	23.96	20.75	100		6.97
			12.14	110	(11.98)	4.61
						3.58
10	Col_{hd} at 22 °C	26.51	22.96	100		7.12
			13.36	110	(13.26)	4.59
						3.83
12	Col_{hd} at 23 °C	27.93	24.19	100		7.18
			14.00	110	(13.97)	4.61
			12.31	200	(12.10)	3.58
14	Col_{hd} at 70 °C	30.25	26.20	100		7.10
			15.17	110	(15.13)	4.68
			13.19	200	(13.10)	3.60
16	Col_{hd} at 70 °C	31.32	27.12	100		7.02
			16.07	110	(15.66)	4.63
			14.00	200	(13.56)	3.63
18	Col_{hd} at 70 °C	32.22	27.90	100		7.03
			16.72	110	(16.11)	4.66
			14.63	200	(13.95)	3.63

The rhodium and iridium series were investigated by variable temperature polarized microscopy and X-ray powder diffraction experiments to determine the structure of the liquid crystalline phase. All the materials displayed a pseudo-leaf-like natural texture with linear birefringent defects indicative of a hexagonal columnar disordered phase (Col_{hd}). These textures were present at room temperature in several of the samples, demonstrating the stability of the liquid crystal phase at room temperature. The assignment of a hexagonal columnar disordered phase (Col_{hd}) was confirmed by the X-ray powder diffraction data obtained at a variety of temperatures. The diffraction data listed in Tables 3 and 4 show the presence of a sharp low angle peak indicative of the (100) reflection of a hexagonal lattice. Lower

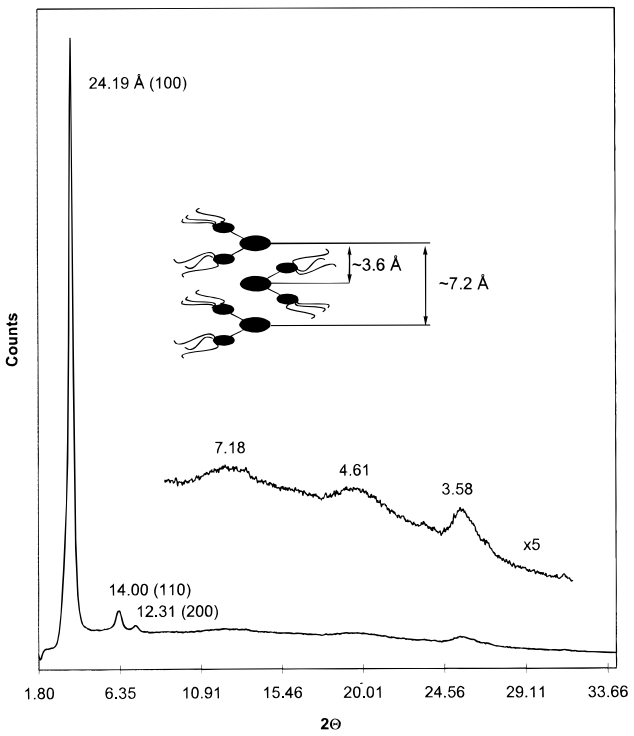

Figure 4. X-ray diffraction pattern of **2**, $n = 12$, at room temperature.

intensity (110) and (200) peaks observed for most compounds provide conclusive proof for the assignment of a hexagonal lattice.

These materials also displayed atypical diffuse scattering. Of particular interest were three broad halos present from the mid-to-high angle region of the diffraction pattern shown in Figure 4. One halo consistently centered around 4.5−4.6 Å is typical of liquid correlations between side chains. The other two halos, centered approximately 3.6−3.8 Å and 7.1−7.3 Å, are due to the liquid-like correlations between the mesogen. The halo centered around 3.6−3.8 Å is the distance between adjacent cores. The second mid-angle halo is indicative of loose correlations at higher length scales and is appropriate for the distance between a mesogen and its second nearest neighbor in the column. To understand this feature, recall that the antiparallel alignment of the nondiscoid shaped material is necessary to produce a disc-shaped dimer for the formation of a columnar phase. This alignment is also favored by dipole considerations. Similar to the well-known cyanobiphenyls, the dipole associated with the carbonyl groups on the metal centers will prefer to have an antiparallel alignment.[4] In other words, the neighboring molecules in the column must be aligned in an antiparallel arrangement in order to prevent the material from exhibiting regions of polarization, which are generally thermodynamically unfavorable.

Further analysis of the X-ray data revealed some interesting properties of the material. A plot of the lattice constant versus the number of carbon atoms in the side chain is linear. Series **1** displays a highly linear relationship ($R^2 = 0.989$) with a slope of 0.974 Å/CH_2 and an intercept of 16.06 Å. Compounds of series **2** similarly have a slope of 0.941 Å/CH_2 and an intercept of 16.30 Å ($R^2 = 0.981$). Furthermore, molecular modeling and published X-ray crystallographic data[5b] were used to estimate the size of **1** with a side-chain length of four carbon atoms. The radius of the half-disc-shaped compound was calculated to be 13.8 Å. The assignment of an antiparallel columnar arrangement for this material is further supported when this calculated radius is compared to the lattice constant for this compound, 19.31 Å, which was determined by X-ray powder diffraction. If the material was aligned as shown in case I in Figure 5, the lattice constant would be slightly more than the calculated radius. If the material was aligned as shown in case III, the lattice constant would be

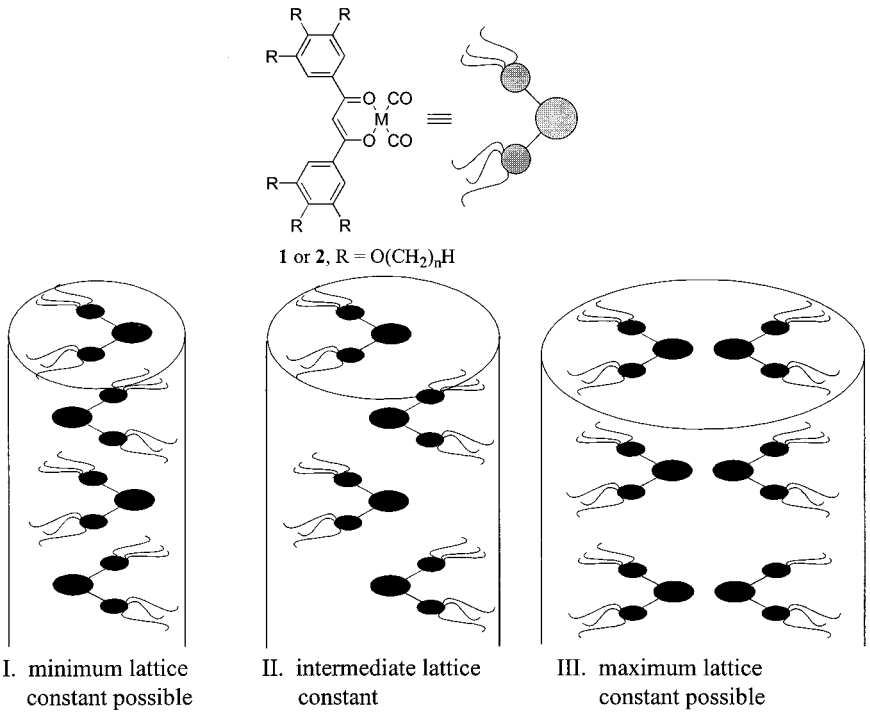

Figure 5. Illustration depicting the possible arrangement of the materials in a columnar phase. See text for discussion.

approximately twice the estimated radius. Since the lattice constant is intermediate between the calculated radius and twice the calculated radius, the material must be aligned in an interdigitated and antiparallel fashion as shown as case II in Figure 5. This alignment is exactly the same as the columnar antiphase proposed earlier for related materials.

The antiparallel alignment of the material was also concluded from miscibility studies with a compound believed to align in such a phase. Compound **9**[3c] has a similar lattice constant (30.15 Å) and mesophase temperature range (50.0−119.3 °C) as **2** with $n = 14$. Both compounds were placed side by side on a microscope slide, heated to the isotropic phase, and then cooled into the mesophase. The area where a mixture of both compounds existed exhibited a decrease in the clearing point but did show a mesophase at 83 °C. Both compounds were freely miscible, and the mixture was liquid crystalline.

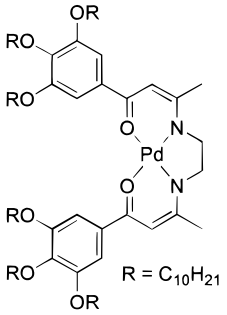

9

Variable-temperature FTIR experiments were conducted in order to probe the degree of metal−metal interactions. The CO stretching frequency provides an excellent probe for observing changes in the electronic environment of the metal due to slight electronic perturbations emanating from changes in the extent of metal−CO back-bonding, which is readily determined from the CO stretching frequency. The compounds investigated were **1** with $n = 12$ and **2** with $n = 14$. The materials were heated to their isotropic phase, and the IR spectrum was recorded at regular temperature intervals throughout the isotropic phase, liquid crystal phase, and solid. The iridium compound showed two sharp peaks at 2066 and 1989 cm^{-1} in the isotropic phase corresponding to the symmetric and asymmetric stretching vibrations. The CO stretching frequencies appeared at 2064 and 1985 cm^{-1} in the liquid crystal and solid phases. These frequencies did not change significantly as hoped when the material was cooled, rather the sharp peaks broadened out and a shoulder appeared at 2047 cm^{-1} as shown in Figure 6. If there were significant metal−metal interactions, it was anticipated that the degree of back-bonding from the metal would decrease causing a shift of the CO peak to higher frequencies. Similar results were obtained with the rhodium sample, which showed two sharp peaks at 2076 and 2005 cm^{-1} in the isotropic phase. These peaks shifted slightly to 2076 and 2002 cm^{-1} in the liquid crystal and solid phase with a shoulder appearing at 2062 cm^{-1}.

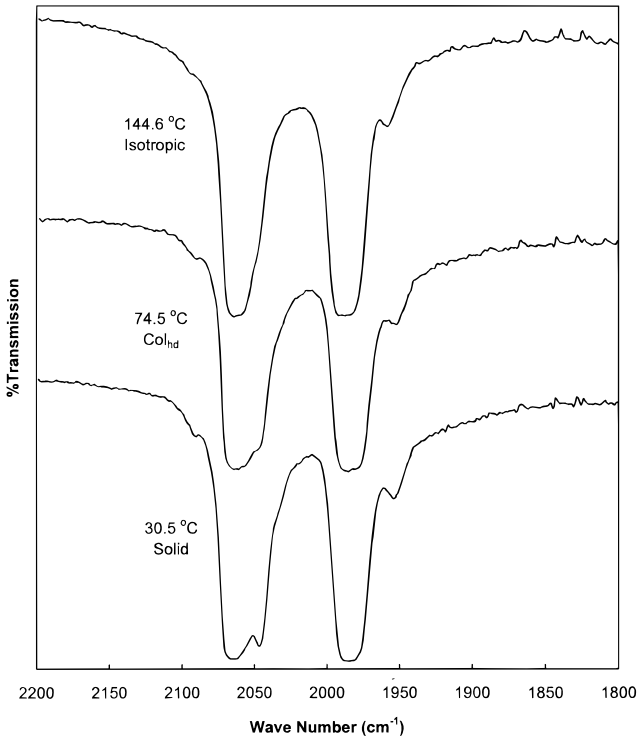

Figure 6. Variable-temperature IR Spectra of **2**, $n = 14$.

Summary

A new liquid crystalline system has been developed incorporating rhodium and iridium centers in a columnar arrangement. These half-disc compounds align in a strict antiparallel arrangement to satisfy dipolar forces producing disc-shaped dimeric units allowing for the formation of a columnar antiphase. These materials display stable liquid crystal phases over a broad temperature range including room temperature. These phases were found to be further stabilized by decreasing the number of carbon atoms in the side chains and by using iridium in the mesogen instead of rhodium.

Experimental Section

General Methods. ^1H NMR spectra were recorded on a Bruker AC-250. ^{13}C NMR spectra were recorded on a Varian Unity VXR 500. Chemical shifts are reported in ppm relative to residual $CHCl_3$ ($d = 7.24$, ^1H; 77.0, ^{13}C). Multiplicities are given as s (singlet), bs (broad singlet), t (triplet), q (quartet), and m (multiplet). Infrared spectra were recorded using a Nicolet Impact 410 FTIR using polystyrene as a standard. Infrared data are reported as s (strong), m (medium), and w (weak). Elemental analyses for carbon and hydrogen were performed on a Perkin-Elmer 240C elemental analyzer and also obtained from Galbraith Laboratories, Inc. Optical characterization was performed using covered microscope slides on a Leica DMRXP polarizing microscope equipped with a Wild Leitz MPS46 Photoautomat along with a Mettler FP 82 HT hot stage and a Mettler FP 80 HT central processor. Variable-temperature infrared spectroscopy was performed by sandwiching a thin film of sample between two 6 mm × 1 mm KBr plates and inserting the plates into the Mettler FP 82 HT hot stage apparatus, which was mounted in the IR beam. Transition temperatures and heats of fusion were determined at scan rates of 10 °C min^{-1} by differential scanning calorimetry using a Perkin-Elmer DSC 7 with a Perkin-Elmer 7700 thermal analysis data station. Variable-temperature X-ray diffraction was measured using Cu Kα radiation on an Inel CPS 120 position-sensitive detector with a XRG 2000 genera-

tor, a fine-focus X-ray tube, and a home-built heating stage. The temperature was regulated with a Minco CT 137 controller with ±1 °C stability. Approximately 2 mg of sample was suspended in 1.5 mm Lindermann glass capillaries. The detector was calibrated using mica and silicon standards obtained from the National Bureau of Standards (NBS). High-resolution FAB mass spectroscopy was performed on a VG analytical ZAB-E instrument using $CHCl_3$ as a solvent with 3-nitrobenzyl alcohol as the matrix.

Unless otherwise indicated, all chemicals and solvents were reagent grade and used as obtained without further purification. Air- and moisture-sensitive reactions were carried out in oven-dried glass ware under an atmosphere of dry argon employing standard Schlenk techniques. Anhydrous tetrahydrofuran (THF), anhydrous diethyl ether (ether), and anhydrous ethyl acetate were purchased from Aldrich in sure seal bottles. Hexane was deoxygenated with argon and stored over 4 Å molecular sieves. Tetracarbonyldi-μ-chlorodirhodium(I) was purchased from Aldrich, and both potassium carbonate and chloro-1,5-cyclooctadieneiridium(I) dimer were purchased from Strem Chemicals, Inc. Potassium hydroxide and anhydrous methanol were purchased from Mallinckrodt. Carbon monoxide was purchased from BOC Gases. All 1,3-bis(3′,4′,5′-trialkoxyphenyl)-1,3-propanedione ligands were synthesized following literature procedures.[7] Throughout the Experimental Section, *n* represents the number of carbon atoms in the alkyl chain.

Dicarbonyl-1,3-bis[(3′,4′,5′-trioctyloxy)phenyl]-1, 3-propanedionatorhodium(I) (General Procedure for 1). This compound was made by adapting a procedure previously reported by Bonati and Wilkinson.[8] Under an argon atmosphere, 0.217 g (0.218 mmol) of 1,3-bis[(3′,4′,5′-trioctyloxy)-phenyl]-1,3-propanedione, 0.151 g (1.09 mmol) of potassium carbonate, and 0.053 g (0.136 mmol) of tetracarbonyldi-μ-chlorodirhodium(I) were combined in a 50 mL Schlenk flask equipped with a condenser. To this flask was added 20 mL of THF, and the reaction mixture was refluxed for 4 h. The THF was removed under reduced pressure, and 20 mL of hexane was added to give a light brown solution. The hexane solution was filtered through a Schlenk frit to remove the inorganic salts, which were then washed with two 10 mL aliquots of hexane. The hexane was removed under reduced pressure, giving an orange-brown oil in a 98% yield. When $n = 12-18$, the product was further purified by recrystallization in ethyl acetate to give an orange solid. All products were moderately air sensitive and should be stored under an inert atmosphere of nitrogen or argon: ^{1}H NMR ($CDCl_3$) 0.86 (t, 18H, CH_3), 1.26−1.46 (m, 60H,$(CH_2)_5CH_3$), 1.70−1.83 (m, 12H, OCH_2CH_2), 3.97−4.04 (m, 12H, OCH_2), 6.66 (s, 1H, COCHCO), 7.06 (s, 4H, ArH); ^{13}C NMR ($CDCl_3$) 14.07, 22.66, 22.68, 26.06, 26.11, 29.28, 29.37, 29.40, 29.51, 30.34, 31.82, 31.89, 69.47, 73.60, 95.56, 106.66, 133.56, 141.87, 152.93, 181.24, 183.39, 183.97; IR (thin film) 2955s, 2920s, 2872s, 2076s (CO), 1999s (CO), 1969w, 1727w, 1586m, 1550s, 1485s, 1468s, 1432s, 1379s, 1344s, 1320s, 1261m, 1232s, 1190m, 1114s, 1007m, 901w, 860m, 777s. Anal. Calcd for $C_{65}H_{107}O_{10}Rh_1$: C, 67.80; H, 9.37. Found: C, 67.69; H, 9.43.

1,5-Cyclooctadiene-1,3-bis[(3′,4′,5′-trioctyloxy)phenyl]-1,3-propanedionatoiridium(I) (General Procedure for *n* = 4−10). Under an argon atmosphere, 0.152 g (0.153 mmole) of 1,3-bis[(3′,4′,5′-trioctyloxy)phenyl]-1,3-propanedione, 0.240 g (1.74 mmole) of potassium carbonate, and 0.056 g (0.083 mmole) of chloro-1,5-cyclooctadieneiridium(I) dimer were combined in a 50 mL Schlenk flask. To this flask was added 20 mL of THF, and the reaction was stirred for 5 h. The THF was removed under reduced pressure, and 20 mL of hexane was added to give an orange solution. The hexane solution was filtered through a Schlenk frit to remove the inorganic salts, which were then washed with two 10 mL aliquots of hexane. The hexane was removed under reduced pressure, giving an orange-brown oil in a 93% yield. ^{1}H NMR ($CDCl_3$) 0.86 (t, 18H, CH_3), 1.26−1.44 (m, 60H, $(CH_2)_5CH_3$), 1.72−1.78 (m, 16H, OCH_2CH_2 and CH_aH_bCH═), 2.30 (bs, 4H, CH_aH_b-CH═), 3.98 (t, 12H, OCH_2), 4.12 (s, 4H, CH_aH_bCH═), 6.58 (s, 1H, COCHCO), 7.05 (s, 1H, ArH); ^{13}C NMR ($CDCl_3$) 14.06, 22.65, 22.67, 26.06, 26.10, 29.28, 29.34, 29.38, 29.50, 23.33, 31.17, 31.81, 31.88, 59.88, 69.40, 73.50, 95.38, 106.62, 122.03, 134.12, 141.65, 152.85, 180.51; IR (thin film) 2956s, 2931s, 2869s, 2844s, 1587m, 1550m, 1519s, 1488s, 1469s, 1431s, 1388s, 1319s, 1231s, 1188m, 1112s, 1000m, 981m, 906w, 869w, 831w, 788m, 719m, 669w, 625w; MS *m/e* 1292 (M^+). Anal. Calcd for $C_{71}H_{119}O_8Ir_1$: C, 65.96; H, 9.28. Found: C, 65.18; H, 9.23.

1,5-Cyclooctadiene-1,3-bis[(3′,4′,5′-tridodecyloxy)phenyl]-1,3-propanedionatoiridium(I) (General Procedure for *n* = 12−18). This compound was made by adapting a procedure previously reported by Whitmore and Eisenberg.[9] Under an argon atmosphere, 0.320 g (0.196 mmol) of 1,3-bis-[(3′,4′,5′-tridodecyloxy)phenyl]-1,3-propanedione was added to a 200 mL Schlenk flask and dissolved in 20 mL of ether. To this solution was added 0.75 mL of a 1 M aqueous potassium hydroxide solution, and the reaction was stirred for 10 min. Chloro-1,5-cyclooctadieneiridium (I) dimer was added, and the reaction was stirred. After 2 h, 30 mL of deionized water was added and the ether removed under reduced pressure, causing the product to precipitate as an orange solid in the water layer. The product was collected by filtration and washed with methanol. The product was purified by dissolving in THF and precipitating it by the slow addition of methanol and collected by filtration in a 90% yield: ^{1}H NMR ($CDCl_3$) 0.86 (t, 18H, CH_3), 1.24−1.45 (m, 108H, $(CH_2)_9CH_3$), 1.69−1.81 (m, 16H, OCH_2CH_2 and CH_aH_bCH═), 2.30 (bs, 4H, CH_aH_bCH═), 3.99 (t, 12H, OCH_2), 4.12 (s, 4H, CH_aH_bCH═), 6.58 (s, 1H, CO-CHCO), 7.05 (s, 1H, ArH); ^{13}C NMR ($CDCl_3$) 14.11, 22.68, 26.09, 26.13, 29.38, 29.36, 29.46, 29.59, 29.67, 29.70, 29.72, 29.75, 30.35, 31.18, 31.93, 59.90, 69.39, 73.52, 95.40, 128.71, 134.13, 141.63, 152.86, 180.52; IR (thin film) 2956s, 2919s, 2850s, 1581m, 1531s, 1488s, 1462s, 1431s, 1375s, 1331s, 1231s, 1188m, 1112s, 1000m, 968m, 950w, 906m, 862m, 775m, 719m, 656w; MS *m/e* 1629 (M^+). Anal. Calcd for $C_{95}H_{167}O_8Ir_1$: C, 70.02; H, 10.33. Found: C, 70.37; H, 10.49.

Dicarbonyl-1,3-bis[(3′,4′,5′-trioctyloxy)phenyl]-1,3-propanedionatoiridium(I) (General Procedure for 2). This compound was made by adapting a procedure previously reported by Whitmore and Eisenberg.[9] Under an argon atmosphere, 0.198 g (0.153 mmol) of 1,5-cyclooctadiene-1,3-bis[(3′,4′,5′-tridodecyloxy)phenyl]-1,3-propanedionatoiridium-(I) was placed in a 25 mL Schlenk tube and dissolved in THF to give an orange solution. Carbon monoxide was bubbled through the solution for 15 min. The solvent was removed immediately under reduced pressure, and the product was dried under high vacuum for 8 h to give an orange-brown oil in a 95% yield. When $n = 14-18$, the compound was recrystallized from ethyl acetate to give an orange solid: ^{1}H NMR ($CDCl_3$) 0.86 (t, 18H, CH_3), 1.26−1.47 (m, 60H,$(CH_2)_5$-CH_3), 1.71−1.84 (m, 12H, OCH_2CH_2), 4.00−4.05 (t, 12H, OCH_2), 6.82 (s, 1H, COCHCO), 7.10 (s, 4H, ArH); ^{13}C NMR ($CDCl_3$) 14.08, 22.66, 22.69, 26.06, 26.11, 29.28, 29.36, 29.38, 29.40, 29.51, 30.48, 31.82, 31.90, 69.57, 73.63, 97.26, 106.79, 132.57, 142.47, 153.08, 169.01, 179.76; IR (thin film) 2961s, 2924s, 2851s, 2730m, 2068s (CO), 1989s (CO), 1721m, 1588s, 1545s, 1466s, 1381s, 1351s, 1320s, 1241s, 1199s, 1120s, 1010s, 895m, 858s, 786s, 713s, 658m, 585w, 530m. Anal. Calcd for $C_{65}H_{107}O_{10}Ir_1$: C, 62.92; H, 8.69. Found: C, 62.39; H, 9.18.

Acknowledgment. We are grateful for financial support provided by the National Science Foundation (DMR-9503572) and the Office of Naval Research.

CM9706098